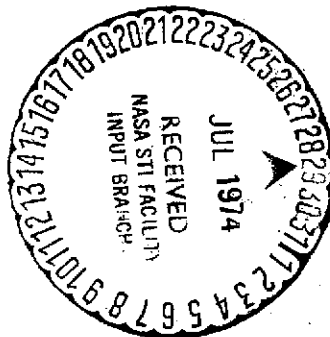


THEORETICAL MODEL OF THE DIURNAL VARIATIONS
OF THE TEMPERATURE, DENSITY, AND WINDS IN
THE EQUATORIAL THERMOSPHERE OF THE EARTH
DURING THE EQUINOX

M.N. Izakov, S.K. Morozov
and E.E. Schnol'

Translation of: "Teoreticheskaya Model' Suto-
chnykh Variatsiy Temperatury, Plotnosti i Ve-
trov v Ekvatorial'noy Termosfere Zemli v Period
Ravnodenstviya," Moscow, Institute for Space
Research, Academy of Sciences USSR, Report
PR-115, 1972, 52 pages



(NASA-TT-F-14663) THEORETICAL MODEL OF
THE DIURNAL VARIATIONS OF THE
TEMPERATURE, DENSITY, AND WINDS IN THE
(Linguistic Systems, Inc., Cambridge,
Mass.) 44 p HC \$5.25

N74-29106

CSCL 04B

G3/20

Unclas
54149

NATIONAL AERONAUTICS AND SPACE ADMINISTRATION
WASHINGTON, D.C. 20546
JUNE 1973

STANDARD TITLE PAGE

1. Report No. NASA TT F- 14,663		2. Government Accession No.		3. Recipient's Catalog No.	
4. Title and Subtitle THEORETICAL MODEL OF THE DIURNAL VARIATIONS OF THE TEMPERATURE, DENSITY, AND WINDS IN THE EQUI- TORIAL THERMOSPHERE OF THE EARTH DURING THE EQUINOX				5. Report Date May 1973	
				6. Performing Organization Code	
7. Author(s) M.N. Izakov, S.K. Morozov, and E.E. Shnol'				8. Performing Organization Report No.	
				10. Work Unit No.	
9. Performing Organization Name and Address LINGUISTIC SYSTEMS, INC. 116 AUSTIN STREET CAMBRIDGE, MASSACHUSETTS 02139				11. Contract or Grant No. NA5002013 NASW-2482	
				13. Type of Report & Period Covered TRANSLATION	
12. Sponsoring Agency Name and Address NATIONAL AERONAUTICS AND SPACE ADMINISTRATION WASHINGTON, D.C. 20546				14. Sponsoring Agency Code	
15. Supplementary Notes Translation of "Teoreticheskaya Model, Sutochnykh Variatsiy Temperatury, Plotnosti i Vetrov v Ekvatorial'noy Termosfere Zemli v Period Ravnodenstviya," Moscow, Institute for Space Research, Academy of Sciences USSR, Report Pr-115, 1972, 52 pp.					
16. Abstract A model of the diurnal variations of the structure and dynamics of the earth's thermosphere is constructed for altitudes of 120-130 km by means of a numerical solution of a system of hydrodynamic equations. The basic features of the model agree with experimental data. A substantial interconnection is shown between the thermal regime and movements. It is found that super-rotation (presence of mean daily west-east wind components) is a consequence of the influence of the daily variations of ion concentrations (due to the slowing down of ions) upon the movement of neutral particles. In the branches of the two-dimensional model arises a shock wave, dividing the area where the gas moves relative to the heat source with supersonic and subsonic velocities.					
17. Key Words (Selected by Author(s))			18. Distribution Statement UNCLASSIFIED - UNLIMITED		
19. Security Classif. (of this report) UNCLASSIFIED		20. Security Classif. (of this page) UNCLASSIFIED		21. No. of Pages 39	
				22. Price	

TABLE OF CONTENTS

	<u>Page</u>
INTRODUCTION	1
I. STATEMENT OF PROBLEM	2
1.1 <u>Initial Equations</u>	2
1.2 <u>Heat Source and Heat Sink</u>	5
1.3 <u>Effect of Ions</u>	7
1.4 <u>Boundaries of Area Examined and Boundary Conditions</u>	10
2. STATEMENT OF COMPUTATIONAL PROBLEM	11
2.1 <u>Features of Numerical Problem</u>	12
2.2 <u>Boundary Conditions</u>	12
2.3 <u>Selection of Initial Data</u>	16
3. COMPUTATIONAL ALGORITHM	16
3.1 <u>Difference Scheme</u>	17
3.2 <u>Organization of Iteration</u>	18
3.3 <u>Linearization of Difference Equations</u>	18
3.4 <u>Solution of One-Dimensional Linear Boundary Problems on a Ray</u>	19
4. RESULTS AND THEIR TREATMENT	19
CONCLUSIONS	24
SUPPLEMENT 1	25
SUPPLEMENT 2	26
SUPPLEMENT 3	27
REFERENCES	38

THEORETICAL MODEL OF THE DIURNAL VARIATIONS
OF THE TEMPERATURE, DENSITY, AND WINDS IN
THE EQUATORIAL THERMOSPHERE OF THE EARTH
DURING THE EQUINOX

M.N. Izakov, S.K. Morozov
and E.E. Schnol'

ABSTRACT. A model of the diurnal variations of the structure and dynamics of the earth's thermosphere is constructed for altitudes of 120-320 km by means of a numerical solution of a system of hydrodynamic equations. The basic features of the model agree with experimental data. A substantial interconnection is shown between the thermal regime and movements. It is found that super-rotation (presence of mean daily west-east wind components) is a consequence of the influence of the daily variations of ion concentrations (due to the slowing down of ions) upon the movement of neutral particles. In the branches of the two-dimensional model arises a shock wave, dividing the area where the gas moves relative to the heat source with supersonic and subsonic velocities.

INTRODUCTION

/3*

In a series of theoretical models of the thermosphere, its thermal regime and dynamics are considered separately, in view of the complexity of the overall problem. Thus, in the models of Harris and Priester [1] and in later analogous models [2,3] in the calculation of diurnal variations of temperature density, the horizontal velocity relative to the earth (wind velocity) was set equal to zero. On the other hand, in calculations of models of global distribution of winds in the thermosphere [4-7], the density and temperature distributions were pre-assigned.

*Numbers in the right-hand margin indicate foreign pagination.

However, from a comparison of the results of calculations from experiments and from theoretical evaluations, it became clear that a sufficiently complete description of the structure and dynamics of the thermosphere is possible only in their interconnection [8-12]. Attempts were undertaken at solutions to this problem with a number of approximations and assumptions [13-16], however the problem is still far from being solved.

In the aforementioned authors' works, a system of equations was formulated which is suitable for a description of the structure and dynamics of the thermosphere [10-12], the function of thermosphere heating by shortwave solar radiation was studied [19-21], and a method is developed for solving this system in two-dimensional space for the description of diurnal variations in the equatorial thermosphere during the equinox [16]. In the present study, results are presented of the solution of a two-dimensional model with a refined heat source and with the effect of ionic friction. The obtained model of diurnal variations agrees in its basic features with experimental data. /4

I. STATEMENT OF THE PROBLEM

I.1. Initial Equations. As was shown in [10-12], the structure and dynamics of the thermosphere may be described by hydrodynamic equations in Navier-Stokes approximations at least to altitudes of 300-500 km (where $K^2 \ll 1$, K being the Knudsen number $K = \lambda/H$, λ being the free path length of the molecule and H , the altitude scale).

In view of the complexity of the overall problem, it is advisable initially to examine the two-dimensional space problem for an equinox period. For this we shall assume a fixed spherical system of ordinates with its origin at the center of the earth (r is the geocentric distance, ϕ is the longitudinal angle from west to east, θ is the latitudinal angle wherein the axis $\phi = 0$,

$\theta = 0$ directed along the earth-sun line) and we shall examine processes occurring in the equatorial plane $\theta = 0$. Then the equations of continuity, motion, internal energy, and equations of state are written in the form [12]:

$$\frac{\partial \rho}{\partial t} + \frac{1}{r^2} \frac{\partial}{\partial r} (r^2 \rho u) + \frac{1}{r} \frac{\partial}{\partial \varphi} (\rho v_\varphi) = 0, \quad (1)$$

$$\rho \left(\frac{\partial v_\varphi}{\partial t} + u \frac{\partial v_\varphi}{\partial r} + \frac{v_\varphi}{r} \frac{\partial v_\varphi}{\partial \varphi} \right) - \frac{1}{r} \frac{\partial \rho}{\partial \varphi} + \frac{\partial}{\partial r} \left(\eta \frac{\partial v_\varphi}{\partial r} \right) + \frac{1}{2} \rho_i \nu_{in} (v_\varphi - u_\varphi), \quad (2)$$

$$\frac{\partial \rho}{\partial r} = -\rho g,$$

$$f c_v \left(\frac{\partial T}{\partial t} + u \frac{\partial T}{\partial r} + \frac{v_\varphi}{r} \frac{\partial T}{\partial \varphi} \right) + \frac{1}{r^2} \frac{\partial}{\partial r} (r^2 \kappa \frac{\partial T}{\partial r}) + \eta \left(\frac{\partial v_\varphi}{\partial r} \right)^2 + \quad (3) \quad /5$$

$$+ \rho \left(\frac{1}{r^2} \frac{\partial (r^2 u)}{\partial r} + \frac{1}{r} \frac{\partial v_\varphi}{\partial \varphi} \right) = Q_{ST} - Q_{IR} + \frac{1}{4} \rho_i \nu_{in} (v_\varphi - u_\varphi)^2, \quad (4)$$

$$p = \rho \frac{R_0}{\mu} T, \quad (5)$$

where t is time, ρ , T , p , u are respectively density, temperature, pressure, and molecular weight of the gas, R_0 is the universal gas constant, η , κ are the coefficients of viscosity and heat conductivity of the gas, ρ_i , v_i are the density and velocity of ions, ν_{in} is the frequency of non-neutral collisions, Q_{ST} , Q_{IR} are the heat source and heat sink, determined below.

We note that these equations are analogous with the equations of the boundary layer [10,12] with the difference that there the pressure is constant in the direction perpendicular to the predominant direction of motion, and here it is variable (with height).

Excluding from consideration the latitudinal coordinate θ , we shall neglect the influence of meridian currents on the processes in the equatorial plane. The feasibility of this assumption is determined by the symmetry of the source Q_{ST} relative to the equator in an equinox period when the subsolar point lies on the equator, as a consequence of which we may assume that for $\theta = 0$, $\partial p / \partial \theta = 0$ and $v_\theta = 0$. Moreover, the simplifying assumption is made that

$\partial v_\theta / \partial \theta = 0$ when $\theta = 0$. The fact that wind calculations are made on more simplified schemes serves as a basis for this, but taking θ into account, the small quantities $\partial v_\theta / \partial \theta$ are yielded in the vicinity of the equator [6,7].

In calculations made thus far, the diurnal variations of the composition of the thermosphere have not yet been taken into account, and therefore the quantities μ , η , κ are taken as functions of altitude from the available experimental data on the altitude distributions of concentrations of basic atmospheric components. Since the diurnal variations of μ in the upper limit does not exceed certain percentages, this simplification cannot significantly change the picture of diurnal variations of ρ , T , v . /6

In view of the fact that the thin layer $\Delta r = 200$ km is examined in comparison with the radius of the earth R_e , the following two insignificant simplifications were made. Firstly, the gravitational force was assumed constant ($g = \text{const}$); secondly, in equations (1-4) terms were omitted which were related to the sphericity of the problem having orders of $\Delta r / R_e$, after which the equations assumed the following form:

$$\frac{\partial \rho}{\partial t} + \frac{\partial}{\partial r} (\rho v_r) + \frac{1}{r_0} \frac{\partial}{\partial \varphi} (\rho v_\varphi) = 0, \quad (6)$$

$$\rho \left(\frac{\partial v_r}{\partial t} + v_r \frac{\partial v_r}{\partial r} + \frac{v_\varphi}{r_0} \frac{\partial v_\varphi}{\partial \varphi} \right) = - \frac{1}{r_0} \frac{\partial \rho}{\partial \varphi} + \frac{\partial}{\partial r} \left(2 \frac{\partial v_\varphi}{\partial r} \right) + \frac{1}{2} \rho_i \gamma_{in} (v_{i\varphi} - v_\varphi), \quad (7)$$

$$\frac{\partial \rho}{\partial r} = -\rho g, \quad (8)$$

$$\begin{aligned} \rho \left(v_r \frac{\partial T}{\partial t} + v_r \frac{\partial T}{\partial r} + \frac{v_\varphi}{r_0} \frac{\partial T}{\partial \varphi} \right) - \frac{\partial}{\partial r} \left(x \frac{\partial T}{\partial r} \right) + 2 \left(\frac{\partial v_\varphi}{\partial r} \right)^2 + \rho \left(\frac{\partial v_r}{\partial r} + \frac{1}{r_0} \frac{\partial v_\varphi}{\partial \varphi} \right) = \\ = Q_{ST} - Q_{IR} + \frac{1}{4} \rho_i \gamma_{in} (v_{i\varphi} - v_\varphi)^2, \end{aligned} \quad (9)$$

$$p = \rho B(r) T, \quad (10)$$

where $B(\tau) = R_0/\mu(\tau)$, $\tau_0 = R_{e0} + h_0$, h_0 being the altitude of the lower boundary of the area examined. /7

I.2. Heat Source and Heat Sink. According to available data, the fundamental heat source in the thermosphere is the energy of the shortwave solar radiation (ultraviolet and x-ray in a range from 30 to 1800 Å). Part of this energy is converted to heat as a result of a large number of elementary processes of interaction of photons with particles of the atmosphere (ionization, dissociation, turbulence, impact deactivation) [19].

We shall assume that for the study of diurnal variations we may disregard slow changes in the volume of the solar flux, since its regular short-term changes have a period of about 27 days. Therefore we may consider the spectral flux of solar radiation $F_{\lambda\infty}$ independent of time and seek a stationary solution of our system of equations (1-5), in the fixed system of coordinates which we are using.

The source of heat, due to absorption of the shortwave solar radiation, Q_{ST} , may be written in the following form [13-21]:

$$Q_{ST}/\eta = \bar{\epsilon}_I \sum_{\alpha} \int_{30\text{Å}}^{1800\text{Å}} F_{\lambda\infty} n_{\alpha} \sigma_{\alpha\lambda} \exp(-\sum_{\alpha} \sigma_{\alpha\lambda} n_{\alpha} H_{\alpha} \sec \chi) d\lambda + \bar{\epsilon}_{II} \int_{1300\text{Å}}^{1800\text{Å}} F_{\lambda\infty} n_{\alpha} \sigma_{\alpha} \exp(-\sigma_{\alpha} n_{\alpha} H_{\alpha} \sec \chi) d\lambda, \quad (11)$$

where $F_{\lambda\infty}$ is the spectral flux of the shortwave solar radiation, n_{α} , H_{α} are the concentration and altitude scales of the α -th component ($\alpha = 1, 2, 3$ since here exist basic components of the thermosphere N_2 , O_2 , O), χ is the zenith angle of the sun (when $\chi > 70^\circ$ instead of $\sec \chi$, a more complex expression is taken [20]), λ is the wavelength, $\sigma_{\alpha\lambda}$ is the cross-section of the absorption of photons by particles of the α -th component. As was shown in [19], we may with good accuracy, set $\bar{\epsilon}_{II} = 0.3$. At the same time, according to approximate evaluations, $\bar{\epsilon}_I = 0.6$, which is also close to the evaluation of Johnson and Gotlieb [22]. /8

In our calculations the flux Q_{ST} was approximated by a function in the form

$$Q_{ST}(\tau) = A \rho \exp(-B \rho T \sec \chi), \quad (12)$$

where the constants A and B were chosen to approximate $Q_{ST}(\tau)$ to an exact ratio given by equation (11).

The heat sink, due to infrared radiation at $\lambda = 63 \mu m$ was taken in accordance with [23] in the form:

$$Q_{IR} = n_0 w_1 A_{12} \frac{w_1 \exp(-w_1/kT) \xi(\tau)}{w_2 + w_1 \exp(-w_1/kT) + w_0 \exp(-w_0/kT)}, \quad (13)$$

where w_α , w_α are the energy and statistical weight of the sub-levels of the fundamental level of the oxygen atom $\tilde{Z}P_{0,1,2}$; A_{12} is the Einstein coefficient; $\xi(\tau)$ is a screening function taking into account secondary absorption of infrared photons; in the given calculation the simplifying assumption was made $\xi = 0.8$ which at the altitudes examined was close to the results of calculations in [24,25].

The form of the ratio Q_{ST}/ρ according to the exact formula (11) and the approximate formula (12) is presented in Figure 1.

Concerning other possible energy sources, calculations show that over the equator in magnetically calm periods, they are small in comparison with the fundamental source Q_{ST} . Blamont's data [26] also confirms this, in that, even at the time of a magnetic storm, changes in temperature in the equatorial region were small although in the auroral regions they were substantial even on magnetically calm days. A certain role may be played, in the lower atmosphere, by energy brought by gravitational waves from the mesosphere [27-29]. The contribution of this source may be

studied within the confines of our model which we also intend to make in the near future; however, in view of the significant divergence of data on its value, still further study is required.

I.3. Effect of Ions. We shall examine in more detail the matter of the effect of ions on the neutral components of the thermosphere, since this effect (the so-called ionic braking or ionic friction), as we shall see below, turns out to be very substantial.

The velocity of the motion of ions in the thermosphere \bar{V}_i may differ substantially from the velocity of the neutral particles \bar{V} due to the interaction of ions with the geomagnetic field \bar{B} . This interaction is described by the Lorentz force entering in the equation of motion for ions, which in rotation together with the earth yields a system of coordinates that may assume the form:

$$\left[\frac{d\bar{V}_i}{dt} = -\frac{1}{\rho} \text{grad} \rho_i + \frac{\rho_i}{\rho} \left(\frac{1}{3} \text{grad} \text{div} \bar{V}_i + \Delta \bar{V}_i \right) - \bar{g} + 2\rho_i (\bar{V}_i \times \bar{\Omega}) + \right. \\ \left. + \frac{e}{m_i} \bar{E} + \gamma_{ni} (\bar{V} - \bar{V}_i) + \omega_i (\bar{V}_i \times \bar{l}_0) \right] \quad (14)$$

where $\omega_i = eB/m_i c$ is the gyrofrequency of the ions; \bar{e}_B is the unit vector in the direction \bar{B} ; \bar{E} is the electric field intensity. Upon the ratio of the two last terms in (14) depends whether ions are entrained by the magnetic field (when $\omega_i \gg \gamma_{ni}$) or by neutral particles (when $\gamma_{ni} \gg \omega_i$). Actually, during examination of large-scale movements in the equatorial ionosphere, the latter two members are basic in value [30], and neglecting the rest and assuming in the equatorial region $\bar{V}_{i\phi} \perp \bar{B}$, we obtain: /10

$$\bar{V}_{i\phi} = \frac{\omega_i \gamma_{ni}}{\omega_i^2 + \gamma_{ni}^2} \left(\frac{\gamma_{ni}}{\omega_i} \bar{V}_\phi - \bar{V}_n \right). \quad (15)$$



Since in the ionosphere at altitudes of h of, 100, 200 and 300 km, respectively, $\omega_i = 160, 190$ and 210 sec^{-1} , and $v_{ni} = 5800, 4$ and 0.5 sec^{-1} [31], then near 100 km, the ions are entrained by neutral particles and at $h \geq 130$ km the ions practically do not move across the lines of force \vec{B} . Since we are considering $h \geq 120$ km, and moreover we are assuming that at $h = 120$ km, $V_\phi = \Omega r_\phi$ (see below), we may assume with a good approximation $V_{i\phi} = \Omega r$, where Ω is the angular velocity of the earth's rotation, i.e. the ions on the average move along the lines of force \vec{B} .

The velocity of the exchange of pulses between particles of different types α and β in a mixture of gases may be described by terms in the form [32, 33]

$$\mathcal{L}_{\alpha\beta} = m_{\alpha\beta} \sigma_{\alpha\beta} v_T n_\alpha n_\beta (\vec{v}_\beta - \vec{v}_\alpha), \quad (16)$$

where $m_{\alpha\beta} = m_\alpha m_\beta / (m_\alpha + m_\beta)$ is the derived mass, $\sigma_{\alpha\beta}$ is the transmission cross section of the pulse, v_T is the average thermal velocity, n_α, n_β are the numerical densities of the particles. The amount of energy transformed into heat in this dissipation process is expressed in the form [33]:

$$R_{\alpha\beta} = \frac{m_\alpha m_\beta}{m_\alpha + m_\beta} \sigma_{\alpha\beta} v_T n_\alpha n_\beta (\vec{v}_\beta - \vec{v}_\alpha)^2. \quad (17)$$

Since we may assume with great accuracy that the mass of the neutral particles and the ions equals $m_i = m_n = m$, then the mass is $m_{in} = m/2$. It is true since we are not considering the composition in detail, we are using the average mass of the neutral particles and the average mass of ions, which in view of the different variations of neutral particle and ion composition with altitude may differ somewhat, but this difference and the error due to this are small. Furthermore, taking into account the condition of quasi-neutrality (which at $h > 100$ km, where the negative ions are extremely few, has the form $n_+ = n_e$ -- the concentration of positive ions is equal to the concentration of electrons), we may obtain for

the interaction of ions and neutral particles from (16) and (17):

$$\mathcal{L}_{in} = \frac{1}{2} \rho \mathcal{G}_{in} \bar{v}_T n_e (\bar{v}_i - \bar{v}), \quad (18)$$

$$\mathcal{R}_{in} = \frac{1}{4} \rho \mathcal{G}_{in} \bar{v}_T n_e (\bar{v}_i - v)^2. \quad (19)$$

The matter of the cross-section of elastic collisions of ions with neutral particles σ_{in} was considered recently in [34,35] in which attention was paid to the polarization of neutral particles by ions and to the process of overcharging. According to [35], the value $v_{in}^* = v_{in}/n = \sigma_{in} V_T \approx 10^{-9} \text{ cm}^3/\text{sec}$ (i.e. approximately an order larger than corresponding value of neutral-neutral collisions), and for collisions of ions with foreign neutral particles, v_{in}^* is not a function of temperature, but for collisions with "native" neutral particles, it depends weakly upon it. Thus, for example:

$$\begin{aligned} v^*(O^+, O_2) &= 1.00 \cdot 10^{-9}, \\ v^*(O^+, N_2) &= 1.08 \cdot 10^{-9}; \quad v^*(O_2^+, N_2) = 0.89 \cdot 10^{-9}; \\ v^*(O_2^+, O) &= 0.75 \cdot 10^{-9}; \quad v^*(O^+, O) = 1.86 \cdot 10^{-9} \\ (T_R/1000)^{0.37}; \quad v^*(O_2^+, O_2) &= 1.17 \cdot 10^{-9} (T_R/1000)^{0.28}; \\ v^*(N_2^+, N_2) &= 2.11 \cdot 10^{-9} (T_R/1000)^{0.38}, \end{aligned}$$

where $T_R = m_{in}(T_i/m_i + T_n/m_n)$. Taking into account these data, we may accept with small error $v_{in}^* = 1.0 \cdot 10^{-9} \text{ cm}^3/\text{sec}$.

The values $n_e(t, h)$ were assigned by means of a certain smoothing of the data of the ionosphere model [36] and excluding nocturnal increases n_e . The function of $n_e(t, h)$ accented in the present calculations is presented in Figure 2.

It should be noted that in [16] the term describing ion friction was strongly overestimated and exerted practically no influence on the solution.

I.4. Boundaries of the Examined Area and Boundary Conditions. The upper boundary of the examined area τ_1 is desirably placed as high as possible in order to completely encompass the processes occurring here; however, it should lie in the region where the hydrodynamic equations are applicable. Moreover, τ_1 should not lie excessively low, so that heat fluxes and mass fluxes acting upon it may be neglected, which substantially simplifies the problem.

From experiments it is known [37,38] that in the thermosphere at altitudes higher than 250-350 km, the temperature ceases to vary with altitude, which (within the limitations of the coefficient of heat conductivity $\kappa(T,u)$) also ensures the absence of heat flux.

We further assume that at sufficiently high altitudes the horizontal component of velocity ceases to vary with altitude.

Thus, we have assumed the following two conditions for the upper boundary:

$$\left. \begin{aligned} \frac{\partial T}{\partial r} \Big|_{\tau_1} &= 0 \\ \frac{\partial v_y}{\partial r} \Big|_{\tau_1} &= 0 \end{aligned} \right\} \quad (20)$$

A third boundary condition is a consequence of the condition of the absence of any mass flux at a sufficiently high altitude. Its mathematical description requires additional treatment which is presented in section 3.2.

The lower boundary τ_0 should be set around 85-90 km, where the diurnal variations of ρ and T are small, according to available experimental data, and where wind velocities are also small in comparison with their velocities in the range of altitudes

examined [37]. However, the presence of complex and insufficiently studied turbulent processes at altitudes $h \approx 105 + 10$ km, makes it ~~advisable in the first stage to study the region~~ h_0 at a high altitude (in the present calculations $h_0 = 120$ km). Then conditions were set for the absence of diurnal variations of ρ and T , and the absence of wind.

$$\begin{aligned} T(\tau_0) &= \text{const}, \\ \rho(\tau_0) &= \text{const}, \\ v_\phi(\tau_0) &= \Omega\tau_0. \end{aligned} \tag{21}$$

It is obvious that an increase in τ_0 somewhat decreases the diurnal variations near the lower boundary of our model.

Some preliminary study of the influence of lower boundary conditions on the solution was conducted by means of a substantial variation of one of them in one of the variants of the calculation, namely the condition $\rho(\tau_0) = \text{const}$ was substituted by: /14

$$v_\tau(\tau_0) = 0.$$

2. STATEMENT OF THE COMPUTATIONAL PROBLEM.

As was already shown, we have assigned a constant flux of solar radiation $F_{\lambda\infty}$ and we are seeking a time-independent solution of the system in (6-10). Such a stationary solution will be constant in time¹. In order to set up a clear mathematical and computational problem, it is necessary to:

(a) assign certain boundary conditions when $\tau = \tau_0$ (on the lower boundary of the layer examined) and when $\tau = \tau_1$ (on the upper boundary);

¹On another possibility, see supplement 2.

(b) select suitable initial data. After this we may expect that the solution of the time problem will approach a certain stationary regime.

2.1. Features of the Computational Problem. Inasmuch as we shall now examine only two basic variables, our (two-dimensional) gas-dynamic problem is rather simple. However, the following radical difference of this problem from the more traditional problems yields a non-trivial computational problem. The density in the interval $\tau_0 \leq \tau \leq \tau_1$ varies by $10^3 - 10^4$ times. The coefficients of the kinematic viscosity (ν) and thermal conductivity (λ) vary by the same amount.

Here in no case should the behavior of 1% (or even 0.1%) of the total mass be neglected. Much to the contrary. The results are more interesting (and more reliable) when the upper boundary is far from the (arbitrarily determined) lower boundary. A second, less significant feature is inherent to all equations of the "boundary layer" type. The system in (6-10) is not a "normal" system of equations with partial derivatives: it cannot be solved relative to the derivatives of the unknown functions in time. These features oblige great care in selecting boundary and initial conditions and leave a substantial imprint on the computational algorithm.

Finally, we note that the problem as a whole has a "closed" character: incipient disturbances are not carried beyond the limits of the region examined. This circumstance increases the time necessary for leaving a stationary regime.

2.2. Boundary Conditions. In the system in (6-10) there are four differential equations, two of which are of the second order in τ . It is necessary, therefore, to have six boundary conditions.

In the lower boundary, when $\tau = \tau_0$, the following three conditions were chosen (see paragraph 1.4):

$$(1) \quad T(\tau_0, \phi; t) = T_0 = \text{const.}$$

$$(2) \quad v_\phi(\tau_0, \phi; t) = \tau_0 \cdot \Omega$$

$$(3a) \quad v_\tau(\tau_0, \phi; t) = 0 \text{ or } (3b) \quad \rho(\tau_0, \phi; t) = \rho_0 = \text{const.}$$

(Ω is the angular velocity of the earth's rotation, (3a and 3b are not equivalent)).

A natural requirement for the positioning of the upper boundary τ_1 is: for further increases in τ_1 the solution should not vary significantly². Thus, a correct statement of the boundary condition above is related to the asymptotic solution of the system in (6-10) when $\tau \rightarrow \infty$.

As we have already stated (see paragraph 1.4), on the upper boundary we assume:

$$\boxed{1) \frac{\partial \tau}{\partial r}(r, \varphi; t) = 0, \quad 2) \frac{\partial v_\varphi}{\partial r}(r, \varphi; t) = 0.} \quad (20)$$

The following considerations elucidate the concept of these conditions. Let us assume that when $\tau \rightarrow \infty$, the restrictions remain:

²In this, of course, we are digressing from the fact that the equations themselves (6-10) are correct to a reasonable accuracy only to a certain altitude h_1 . In an ideal mathematical problem, the equations are naturally considered in the region $\tau_0 \leq \tau < \infty$, but for an interpretation of the results, the region is restricted to

$$\tau_0 \leq \tau \leq R_e + h_1.$$

$$a) \frac{1}{\rho} \frac{\partial}{\partial r} \left(x \frac{\partial T}{\partial r} \right) \text{ in (9), by } \frac{1}{\rho} \frac{\partial}{\partial r} \left(\rho \frac{\partial v_r}{\partial r} \right) \text{ in (7)}$$

Then $\left[\frac{\partial}{\partial r} \left(x \frac{\partial T}{\partial r} \right) \text{ and } \frac{\partial}{\partial r} \left(\rho \frac{\partial v_r}{\partial r} \right) \text{ exponentially} \right] \rightarrow 0.$

Hence: $\left[x \frac{\partial T}{\partial r} \rightarrow J_1(\varphi, t); \rho \frac{\partial v_r}{\partial r} \rightarrow J_2(\varphi, t) \right]$

(also exponentially rapidly).

The convergence of the heat and the pulse³ fluxes to zero yields: $\tau_1 = \tau_2 = 0$. Finally, for a constant composition and temperature $\rho \rightarrow \rho_\infty (\neq 0)$, $x \rightarrow x_\infty (\neq 0)$ and, this means that when $\tau \rightarrow \infty$, it is necessary that

$$\frac{\partial T}{\partial r} \rightarrow 0, \quad \frac{\partial v_r}{\partial r} \rightarrow 0.$$

Thus, (20) simulates the absence of fluxes through the upper boundary for the heat and (horizontal component) pulse. For simulating the conditions of the absence of mass flux: /17

$$\lim_{\tau \rightarrow \infty} \rho(r, \varphi, t) v_r(r, \varphi, t) = 0 \quad (22)$$

knowledge of the asymptotic behavior of ρ and v_r is required. For ρ it is obvious: when $\tau \rightarrow \infty$ the density ρ diminishes exponentially. More accurately, if $T \rightarrow T_\infty$ and the molecular weight $M \rightarrow M_\infty$, then:

$$\rho(r, \varphi, t) = \exp(-a\tau + b + \epsilon_1); \quad a = a(\varphi, t); \quad b = b(\varphi, t) \quad (23a)$$

or

³The tensor components of the pulse flux is: $\Pi_{rz} = \rho v_r v_z + \rho \frac{\partial v_r}{\partial r}$

$$\left[\begin{aligned} b(r, \varphi, t) = \ln \frac{p}{p_0} = -a(\varphi, t)r - \tilde{b}(\varphi, t) - \varepsilon(r, \varphi, t) \\ \varepsilon \rightarrow 0 \quad \text{for } r \rightarrow \infty \end{aligned} \right] \quad (23b)$$

The velocity v_r behaves more precisely. Namely, during the satisfaction of equation (22), v_r linearly approaches ∞ .

$$\left[v_r(r, \varphi, t) = a_1(\varphi, t)r + b_1(\varphi, t) + \varepsilon_1(r, \varphi, t) \right] \quad (24)$$

Taking into account (24) (see supplement 1), we select as the final (sixth) boundary condition:

$$\left[\frac{\partial^2 v_r}{\partial r^2}(r, \varphi, t) = 0 \right] \quad (25)$$

We note that (22) follows in turn from (24) and (23).

Thus the boundary condition (25) which we have set is an approximate description of requirement (22) -- the absence of mass flux at infinity.

NOTES

1. It is not mathematically obvious where it is necessary to place the inadequate boundary conditions. A model examination of this problem (in linearized equations and in fixed coefficients) and numerical experiments consistently demand one more condition above, but not below.

2. The trivial substitution of (22) in the condition $\left. \frac{\partial v_r}{\partial r} \right|_{r=\tau_1} = 0$, as may easily be seen, is inadmissible.

3. Condition (25) contains a second derivative; equations (6-10) contain only the first derivative $\partial v_r / \partial r$. In this sense (25) is a non-standard condition. We note that the asymptotic (24) is typical even for ordinary equations of the boundary layer (where p is not a function of r), but there the problems of the sixth boundary condition do not arise.

2.3. Selection of Initial Data. Excluding the pressure ($p = B(\tau) \cdot \rho \cdot T$) in equations (6-9), we obtain a system of four equations for four unknown functions ρ , T , v_τ and v_ϕ . $\partial v_\tau / \partial \tau$ does not enter them. It is clear, therefore, that one may not assign v_τ arbitrarily when $t = 0$. Further, ρ and T in each moment of time (including even when $t = 0$) are related by the relationship in (8).

Therefore as initial conditions for system (6-9), it is sufficient to assign two functions $T(\tau, \phi; 0)$ and $v_\phi(\tau, \phi; 0)$ and the value of the density in the lower boundary $\rho(\tau_0, \phi; 0)$ when $t = 0$.

In order to accelerate the determination process it is desirable to have a preliminary coordination of the temperature profiles and heat-evaluation. We selected the initial data by the following means. For each variant we preliminarily solved a simplified problem in which the horizontal winds are absent (see supplement 2). The solution of this problem-function $T(\tau, \phi) \cdot \rho(\tau_0, \phi)$ is used as the initial data. It is further assumed that $v_\phi(\tau, \phi, 0) \equiv \tau_0 \cdot \Omega$. The determination time is, with a reasonable degree of accuracy⁴ from 10 to 30 days.

3. COMPUTATIONAL ALGORITHMS

Equations (6-9) are rewritten for the variables v_ϕ , v_τ , T , σ ($\sigma = \ln \rho / \rho_0$). Later, for numerical solution, the differential equations were replaced by the differences. A simpler double-layered implicit difference scheme was used. More accurately, the quantities v_ϕ , T , σ were assigned to the "integral" layers $t = t_n$, and the quantity v_τ was assigned to the semi-integral layers $t = t_n + x/2 = t_n + \tau/2$. The difference scheme is

⁴For example, $|T(t_n + \text{days}) - T(t_n)| < 0.01 T(t_n)$.

formally implicit: for determination of the quantities T^{n+1} , v_ϕ^{n+1} , σ^{n+1} , $v_\tau^{n+1/2}$ (for the known T^n , v_ϕ^n , σ^n), we obtain a system of nonlinear difference equations. It is solved by iteration wherein the terms corresponding to the angular derivatives are taken from the aforementioned iterations. Thus, in fact, we have in angular variables more or less complex (as a function of the number of iterations) implicit schemes with all of the resultant consequences.

Let us dwell briefly on several details.

/20

3.1. Difference Scheme. For an approximation of the derivatives along the vertical in equations of the second order (7) and (9), an implicit six-point scheme was selected. The difference approximations are:

$$\frac{\partial f}{\partial \tau} \approx \frac{1}{2\Delta\tau} \left[(1-\beta)(f'_{m+1} - f'_{m-1}) + \beta(f''_{m+1} - f''_{m-1}) \right]; \quad \beta \leq \frac{1}{2}. \quad (26)$$

$$\frac{\partial^2 f}{\partial \tau^2} \approx \frac{1}{(\Delta\tau)^2} \left[(1-\beta)(f'_{m+1} - 2f'_m + f'_{m-1}) + \beta(f''_{m+1} - 2f''_m + f''_{m-1}) \right]. \quad (27)$$

Here the upper index "I" designates that the quantity is taken at the upper layer $t_n + \tau$, and the index "0" from the layer t_n . For equation (6), an implicit four-point scheme was used. Equation (8) (on each layer) is written for two neighboring points.

The system is vertically non-uniform: the points bunching up downward⁵.

The angular derivatives are approximated analogously.

⁵More accurately, instead of τ , $z = z(\tau)$ ($z'(\tau_0) \gg z'(\tau_1)$) is used. The z -spacing is constant.

In the derivatives of the example, the calculations were conducted on a 25 by 20 network for " ϕ " and " τ ", respectively.

3.2. Organization of Iterations. In the recurrent " $S + 1$ " iteration, the "angular" derivatives $\partial f / \partial \phi$ are taken from the aforementioned iterations. More accurately:

$$\left(\frac{\partial f}{\partial \psi} \right)^{(S+1)} \approx \frac{1}{2\Delta\psi} \left[(1-\alpha)(f_{k+1}^{(S)} - f_{k-1}^{(S)}) + \alpha(f_{k+1}^{(0)} - f_{k-1}^{(0)}) \right]$$

Thus a system of nonlinear difference equations in the given iteration degenerates into a one-dimensional system on each "ray" $\phi = \phi_k$. Corresponding one-dimensional boundary problems are solved by several internal processes of successive approximations --by iteration of " τ ". The system may be stable (by linear criteria) if the number of iterations $S_{\max} \geq 2$. For $S_{\max} = 2$, the condition of stability is:

$$\frac{\tau}{\tau_0 \Delta\psi} |\psi_p \pm a| \leq \sqrt{\frac{2\alpha-1}{\alpha}},$$

where a is the speed of sound.

3.3. Linearization of difference equations. The one-dimensional difference system on the ray ideally (inasmuch as the known quantities are close to the initial values of the aforementioned layer) should be solved by Newton's method--with complete linearization in each iteration. It is known that such a complete linearization is almost never done, since it leads to a boundary problem for a system of engaged linear equations. In our case, the equations are very strongly connected⁶, so that the simultaneous solution of linear equations is unavoidable. Therefore we shall produce a practically complete linearization. For example,

⁶One of the reasons for this is the absence of a derivative with respect to " t " in equation (8).

in the successive j -th iteration member, the corresponding member in difference equations $u(\partial\sigma/\partial\tau)$ is written in the form:

$$\left(u \frac{\partial \sigma}{\partial \tau} \right)^{(j)} = u^{(j)} \left[\frac{\partial \sigma}{\partial \tau} \right]^{(j-1)} + u^{(j-1)} \left[\frac{\partial \sigma}{\partial \tau} \right]^{(j)} - u^{(j-1)} \left[\frac{\partial \sigma}{\partial \tau} \right]^{(j-1)}$$

Here $[\partial\sigma/\partial\tau]$ is the corresponding resonance operator.

3.4. Solution of Uniform Linear Boundary Problems on a Ray.

/22

The system of linear difference equations solved in the j -th internal iteration (according to τ) consists of two equations of the first order and two equations of the second order. As each (well-defined) system of difference equations, it may be solved by the exclusion method with the selection of the main element by column, or using some other universal algorithm. We used a certain variant of the exclusion method in which the order of exclusion is prescribed⁷. Such an algorithm is more economical, however its suitability in the final analysis is verified experimentally.

4. RESULTS AND THEIR TREATMENT

Two conditions were considered--the first for high and the second for low solar activity. In the first case the flux $F_{\lambda\infty}$ measured by Hinteregger [39] was used for a medium-high solar activity corresponding to a flux of the decimetric solar radiation $F_{10.7} = 150 \cdot 10^{-22}$ watts/m²·Hz. For low solar activity there are not now such reliable values of $F_{\lambda\infty}$, since in [39], the results of the aforementioned author are placed in doubt. Therefore for low solar activity, a value of $F_{\lambda\infty}$ was taken in which the current in the ionization continuum was for each value of λ one-half that of the first case. Of course this is a rather crude approximation since the variations of spectral flux in solar

⁷See supplement 3.

activity are extremely complex [39,40].

The diurnal variations of temperature and density at altitudes of 320 and 150 km are represented in Figure 3, where complex curves plot the basic variant, the dot-dash curves plot the variant with ion friction, 1/10-th the normal, the dots plot the variant without horizontal motion ($v_\phi = 0$); moreover, the dotted lines show the variations with additional viscosity, the meaning of which will be shown below. The altitude profiles T and ρ for the first case are presented in Figure 4.

From Figures 3 and 4 it is evident that the temperature at 320 km in the area of the isotherm varies from 900 to 1000 to 1200 to 1300 K, and the density, for example, from $2.5 \cdot 10^{-14}$ to $5 \cdot 10^{-14}$ g/cm³. At 150 km the variation is significantly less; however, we remember that it may be somewhat reduced here due to approximate boundary conditions at 120 km.

It is also evident that the maximum temperatures and densities occur at the same time. Great diversification of phases during certain hours is not observed⁸. We note immediately that it is true that this result is obtained without taking into account the dynamic influence of the mesosphere.

An important conclusion may be drawn from a comparison of the data of the different variants: there exists an extremely strong influence of the motion (including ion motion) upon the thermal regime of the thermosphere producing it. Actually, if there were no winds the thermosphere would heat up practically to sunset (dotted line) and for stronger winds which would

⁸Such diversification of phases was assumed for the agreement of data on the diurnal course of density according to the braking of the satellites and on the diurnal course of temperature according to incoherent scattering (see for example [41]).

develop during low ion friction, the maximum T and ρ would be close to midday (dot-dash line), then for the most probable conditions (solid line) the maximum T and ρ lie in 16-17 hours, which is close to experimental data obtained by the method of incoherent radiowave scattering [42-44].

/24

As a consequence of this influence, there is also a second important fact: the shape of the curves describing the diurnal variations including the positions of maxima and minima may vary for a change in conditions. Actually, the random variations of the source and as a result, variations of wind, and also the ion concentration--all this reflects on the variations of ρ and T . (This is, as it were, the "weather" of the thermosphere as contrasted with "climate", describing the most probably function). For example, for ion braking amounting to 1/10-th the normal (the dot-dash line), significantly earlier maxima of T and ρ take place--around 13 hours--and a noticeably differing form of the diurnal course (a very broad, almost symmetrical T , a sharper maximum ρ , with a more rapid falling off of the latter after the maximum; this also takes place to a lesser degree in the basic variant). Reverse tendencies from the most probable diurnal course are possible; for example, for an increase in the ion concentration, the maximum will be shifted to a later time and the arbitrary course will approach the dotted line.

The fact of the variability of the shape of the diurnal variation curves and of the position of the maxima confirms well the data of incoherent scattering and several other experimental results [42-44]. Also the absolute temperature value obtained in these calculations [44] satisfactorily agree with experimental data, while the values of density are somewhat higher than those in [38], probably due to the approximation of $u(h)$.

The interesting diurnal variations of wind obtained in the model (Fig. 5--dependent upon time at altitudes of 320 and 150 km; Fig. 6--altitude profiles for maxima and minima: winds from

/25

east to west with velocities of 30-150 m/sec prevailing in the morning and during the day (to the maximum of ρ and T) shift in the east-west direction with velocities to 300-350 m/sec. As a consequence of this the average daily velocity v_ϕ is directed from west to east. This fact was noted by King-Hele according to the variations of the slope of the satellite orbit [45-47] and which he called super-rotation (since this fact signifies that the atmosphere at these altitudes on the average surpasses the rotation of the earth). From these data it follows that the reason for super-rotation (in any case, the basic reason) is the influence of daily variations in the ion concentration through ion breaking: the large ion concentration in the day leads to a larger decrease in the daily values of winds than those of the night, and the latter are directed from west to east. This explanation affirms the data of the first variant of our calculations [16] where the virtual absence of ion breaking produced an absence of super-rotation. The ratio of the mean daily velocity of rotation of the atmosphere to its rotation velocity as a whole together with the earth at an altitude of 320 km in our model is $\Lambda = 1.15 - 1.2$, and according to the data of King-Hele, $\Lambda = 1.3$ [47]. At an altitude of 150 km, in both cases, $\Lambda \approx 1.1$ (see Fig. 7).

The vertical velocities v_z are directed upward during the day and downward during the night, and reach 2 m/sec. They strongly affect the thermal regime: adiabatic heating and cooling of the gas during its lowering and rising in the gravitational field of the earth with such velocities is comparable to the heating of solar radiation. In particular, adiabatic heating during the descent of the gas may explain the somewhat slower decrease in T after the maximum in comparison with ρ , and also the beginning of the entries of T after the minimum even at night when the solar source is absent.

/26

One more feature of the diurnal variations of winds in our model which have already been noted in [16] is the formation of

shock wave where the mach number calculated by the velocity of motion of the gas relative to the heat source ($v_\phi + \Omega_1$) is greater than one. Such a shock wave takes place at around 0-3 hours.

Due to the presence of the shock wave a complete determination was not managed, and the calculation was conducted up to the formation of the shock wave.

A complete determination was obtained in a calculation with additional viscosity which may be introduced on the basis of the following hypothesis. Since the motions in the thermosphere take place with large Reynolds numbers ($Re = 10^7 - 10^4$ as a function of altitude), consequently the motions may be unstable and large-scale turbulence may arise. We note that large-scale two-dimensional turbulence in the troposphere (the elements of which are cyclones and anti-cyclones) were studied in articles [48, 49]. Blamont's data [26] treats the possibility of the existence of large-scale two-dimensional turbulence in the thermosphere which, measured with a satellite, the temperature at an altitude of about 260 km, detected its irregular variations on the order of ± 200 degrees (contributing to the diurnal variations), formed in an area with a space scale on the order of 10^4 km. If the temperature fluctuations are interpreted as a reflection of the large-scale two-dimensional turbulence with a characteristic space scale $L \sim 10^9$ cm and a characteristic velocity $V \sim 5 \cdot 10^3$ cm/sec as a consequence of this the coefficient of turbulent viscosity is taken as $V_T \sim LV \sim 5 \cdot 10^{12}$ cm²/sec, substituting in equation (2) the member $\frac{V_T}{\tau_o^2} \cdot \frac{\partial v_\phi}{\partial \phi^2}$, then a variant is obtained (represented by the dotted line in Fig. 3-6), in which the shock wave disappears but in the remainder the figure does not substantially change. This variant was calculated to the complete determination of the periodic regime, which, as noted above, occurred for 10-15 days.

In the calculations presented the effect of change of the lower boundary conditions was studied: two variants were tested: 1) $\rho(\tau_o) = \text{const}$; 2) $v_T(\tau_o) = 0$. The first condition seems to be more

justified, although, as is known, it is best fulfilled at around 90 km [37]. A comparison of these two variants shows that the influence of such variation of conditions on the lower boundary is very substantial at an altitude of 150 km and negligibly small at 320 km.

The results of calculation of the second condition for low solar activity are shown in Figs. 8 and 9. Here also are obtained temperature values close to the experimental values from 600 to 800°K (cf. [43]); there are also some exaggerations of density in the upper part of the altitude range examined.

CONCLUSION

On the basis of the results of calculations presented and comparisons of these with the experimental data, it seems possible to draw the following basic conclusions on the diurnal variations in the atmosphere:

1. There exists an extremely strong interconnection between horizontal and vertical motion of gas (including the motion of ions) and variations of temperature and density in the thermosphere.
2. There is a mean daily west-east component of velocity (super-rotation phenomenon), being a consequence of the influence of the diurnal variations in the ion concentration to ion breaking /28 upon the motion of neutral particles.
3. The motions induced variations in the shape of curves describing the diurnal variations of temperature and density wherein the maximum may for different conditions shift from its most probable position by several hours both to earlier hours and to later hours. The most probable position of the maximum of the diurnal course of temperature and density is 15-17 hours; the minimum is at 2-3 hours local time.
- A substantial difference in the phase of diurnal variations of temperature and density is unlikely. Yet, if it does take place, its cause may be a dynamic influence of the mesosphere.
4. In the two-dimensional model, in the diurnal distribution of wind, a shock wave is produced in the area where the gas moves relative to the peak force, with supersonic velocities. Shock waves disappear in the presence of a large-scale horizontal tur-

bulence (although the area of large horizontal wind gradients remains).

5. As a comparison of experimental and calculated temperature values indicates, the fuller short-wave radiation is the basic heat source in the equatorial thermosphere in the magnetically calm periods.

SUPPLEMENT 1

/29

Notation (with no strict pretension to rigorousness) the derivation of formulas (23) and (24).

From (8) and (10) we have $\zeta = \ln \frac{p}{p_0} \quad (p_0 = p(0, \varphi, t))$

$$\frac{\partial \zeta}{\partial \varphi} = -\frac{g}{BT} - \frac{1}{T} \frac{\partial T}{\partial r}$$

or

$$\zeta(r, \varphi, t) = -\frac{g}{B_\infty T_\infty} r - \ln \frac{T}{T_0} + g \int_{r_0}^r \left(\frac{1}{B_\infty T_\infty} - \frac{1}{BT} \right) dr.$$

Hence

ε (23)

$$|\varepsilon(r, \varphi, t)| = \ln \frac{T}{T_\infty} - g \int_{r_0}^r \left(\frac{1}{B_\infty T_\infty} - \frac{1}{BT} \right) dr.$$

It may be shown that ε approaches zero exponentially:

$$|\varepsilon(r, \varphi, t)| \leq C(v, t) \cdot \exp(-\alpha r)$$

Further, from the discontinuity equation (6):

$$\frac{\partial \zeta}{\partial t} + \frac{1}{r_0} \frac{\partial v_\varphi}{\partial \varphi} + \frac{v_\varphi}{r_0} \frac{\partial \zeta}{\partial \varphi} + \frac{\partial v_r}{\partial r} + v_r \frac{\partial \zeta}{\partial r} = 0.$$

Inserting (23)*, we obtain

$$\frac{\partial v_r}{\partial r} - (a + \varepsilon_2) v_r = A r + B + \varepsilon_3.$$

here

$$A = \frac{\partial a}{\partial t} + v_\infty \frac{\partial a}{\partial \varphi}, \quad B = \frac{\partial b}{\partial t} + v_\infty \frac{\partial b}{\partial \varphi} - \frac{\partial v_\infty}{\partial \varphi} \quad (a, b \text{ from (23)})$$

*We are assuming, of course, that the asymptotic formulas may be differentiated with respect to t and to ϕ .

Hence

$$\tilde{u}_i = \exp(a\tau) \left[\int_{\tau_0}^{\tau} \tilde{E}_2(\tau, \varphi, t) d\tau \right] \left[\left(\int_{\tau}^{\infty} (A\tau + B + E_3) \exp(-a\tau) d\tau - \int_{\tau_0}^{\tau} \tilde{E}_2(\tau, \varphi, t) d\tau \right) \right].$$

Condition (22) yields: $C = 0$.

/30

For the remaining unique solution:

$$\tilde{u}_i(\tau, \varphi, t) = a_i(\varphi, t) + b_i(\varphi, t) + E_i(\tau, \varphi, t).$$

Here $a_i = -A/a$, $b_i = -\frac{A+ab}{a^2}$. All ε_2 (exponentially) approach zero for $\tau \rightarrow \infty$.

SUPPLEMENT 2

For finding the stationary solution of the system (6-10) it seems possible to proceed thus. Set immediately the derivatives with respect to time equal to zero and for the system obtained solve the Cauchy problem for ϕ - since this is done in the theory of the stationary boundary layer.

In such a process the variable ϕ plays the role of time, so that this numerical problem is spatially one-dimensional, i.e. much simpler than the overall (non-stationary) problem.

Here, of course, one should not be restricted to finding solutions in the interval $0 \leq \phi \leq 2\pi$, but some number of evolutions should be made for obtaining functions periodic in ϕ .

We made a detailed attempt in the first stage of the work. It turned out that in this manner it is possible to find a solution which is a continuous function of ϕ . A solution containing shock waves may not be found in this manner, and we necessarily returned to an examination of the non-stationary equations (6-10).

We note that the "motion relative to ϕ " procedure is always applied in the solution of a simplified variation of the problem - for the absence of horizontal winds. We select from the system (6-10) equation (7) and set $v_\phi = \Omega \cdot \tau_0$ in the remaining equation. Then the stationary solution in which we are interested is satisfied by equations

/31

$$\begin{cases} \Omega \frac{\partial P}{\partial \varphi} + \frac{\partial (P v_r)}{\partial r} = 0, \\ \rho c_v \left(\Omega \frac{\partial T}{\partial \varphi} + v_r \frac{\partial T}{\partial r} \right) + P \frac{\partial v_r}{\partial r} - \frac{\partial}{\partial r} \left(\kappa \frac{\partial T}{\partial r} \right) = Q_{ST} - Q_{IR}, \\ \frac{\partial P}{\partial r} = -\rho g \quad P = B(r) \rho T. \end{cases} \quad (S-1)$$

A solution of this system was obtained with sufficient accuracy for 10-15 complete evolutions.

The functions obtained were used as initial conditions in solution of the overall system (6-10).

/31

SUPPLEMENT 3*

Solution of One-Dimensional Difference Boundary Problems

1. In the solution of the boundary problem where a system of linear difference equations, a transposition of boundary conditions is performed implicitly or explicitly. We remember the idea of boundary conditions transposition in the example of the one-dimensional system of difference equations of the first order:

$$\boxed{A_k \bar{u}(x_{k+1}) + B_k \bar{u}(x_k) = 0, \quad k=0, 1, \dots, K.} \quad (S-2)$$

Here A_k and B_k are matrices, $x_k = a + kh$, \bar{u} is the n -dimensional vector: $\bar{u} \in \mathbb{R}^n$.

We may arbitrarily define $u_{(xk)} \in \mathbb{R}^n$ for some k and $\bar{u}_{(x)}$ will be completely determined**.

Now let some linear boundary conditions be given: e at the left ^{/32} ρ at the right ($e + \rho = n$). We shall examine all solutions of (S-2) satisfying the left boundary condition. They form a linear space*** of dimension $n - e = \rho$. The same values of these solutions in the points $x_k - U(x_k)$ are not arbitrary but belong to some space $R_{\rho}(x_{k+1})$.

*Calculated on a special computer.

**It is assumed that A_k and B_k are non-degenerate.

***More exactly, for non-uniform boundary conditions - a hyperplane (not passing through zero).

Equation (S-2) makes it possible, by knowing $R \rightarrow (x_k)$, to find $R \rightarrow (x_{k+1})$ and in the same way to retrace the influence of the left boundary conditions on the whole segment (a, b) . When $k = K$ we obtain:

- 1) $U(x_k) \in R^p \rightarrow (x_K)$ as a consequence of the left boundary conditions;
- 2) $U(x_K)$ satisfies ρ , with the right boundary conditions.

Hence $\overline{U}(x_k) = \overline{U}_k$ is found.

Now, using (S-2), we may successively find

$$\overline{U}_{k-1}, \overline{U}_{k-2}, \dots, \overline{U}_1$$

We shall leave here without treatment of the computational stability of the described procedure. We note only that for an "inverse course" in the general case it is necessary to avoid going out (as a result of errors of rounding off) of the spaces $R \rightarrow (x_k)$: beyond these spaces the solution of the Cauchy problem (from right to left) is unstable.

2. The clearest idea of boundary conditions transfer results in conditions where the space $R \rightarrow (x_k)$ is found explicitly. In this the duality may obtain:

- a) Let $R \rightarrow (x_k)$ be the "basis"*
- b) Let $R \rightarrow (x_k)$ be assigned as a system of equations.

In the case a) one should see to it that the bases are not too obliquely angled. A corresponding process was suggested and founded by Godunov (see [50 and 51]). /33

Method b) is realized for a very extended particular case: one difference equation of a second order?

$$\left. \begin{aligned} a_k u_{k-1} + b_k u_k + c_k u_{k+1} &= f_k, \\ u_0 &= \alpha; \quad u_N = \beta. \end{aligned} \right\}$$

Equation (S-3) may be rewritten in the form of a system of

*The entire $P+1$ vector: one of the hyperplanes and p lie in the space parallel to it.

two equations of the first order (S-2), setting

For (S-3) a method of solution called the "die" method (cf. [52]) is often used.

In the first stage of this method a recurrent relation is sought as a consequence of the left boundary condition:

$$\boxed{U_{\kappa} = q_{\kappa} U_{\kappa+1} + \gamma_{\kappa} \quad , \quad \kappa=0, 1, \dots, K-1.} \quad (S-4)$$

In the second stage, from (D-4), U_{κ} is found in the series

$$\boxed{K, K-1, \dots, 0.}$$

Rewriting (D-4) in the form

$$\boxed{-\tilde{U}_{\kappa+1} = (q_{\kappa} - 1) U_{\kappa+1} + \gamma_{\kappa}}$$

, we see that (S-4) is an equation of the space $R \rightarrow (x_{\kappa+1})$ in the given case, a line in the two-dimensional space R^2 .

On the other hand, we note that the "die" method is a variation on the exclusion method for system (S-3) considered simply as a system of linear equations. More accurately, this is the simplest method of exclusion in which transposition of equations for unknowns is not done.* This observation makes it possible /34 to regard the entire problem somewhat differently.

3) The system of linear difference equations with (linear) boundary conditions behaves as the sum of of the specific system of linear equations. It gives us some "reliable" method of solving linear systems satisfying the requirement for the necessary quantities of calculations proportional to the number of points (and not K^2 or K^3).

Such a requirement satisfies the Gauss exclusion method with a selection of the main element by column. Undoubtedly, it is suitable for the solution of any well-established difference boundary problem for a not-too-large K^{**} .

*Therefore the "die" is suitable to problem (S-3) not for all $a_{\kappa}, B_{\kappa}, C_{\kappa}$.

**The role of errors of curvature for large K is needed in a separate study (cf. Sect. 38 with Ref. 52).

The direct course of the method of exclusion is, in this, an analog to the "transfer of boundary conditions" from left to right, although the $R_{\rightarrow}(x_k)$ are in explicit form and do not appear.

4) We shall write the algorithm used for our problem.

For the chosen linearization* on the ray in each "internal iteration" we obtain a system of three related and different equations for v_1 , T , b and a separate equation for v_ψ .

This equation of the type (D-3) is easily solved by the die method. A system of three different equations corresponding to equations (6), (8), and (9) is obtained. $v_1 = U$ is written in the form:

$$1) \kappa_{16} \delta_m + L_{16} \delta_{m+1} + \kappa_{1u} u_m + L_{1u} u_{m+1} + D_1 = 0, \quad (S-5.1)$$

$$2) \kappa_{26} \delta_m + L_{26} \delta_{m+1} + \kappa_{2T} T_m + L_{2T} T_{m+1} = 0, \quad (S-5.2) \quad /35$$

$$3) A_T T_{m+1} + B_T T_m + C_T T_{m+1} + A_u u_{m+1} + B_u u_m + C_u u_{m+1} + B_\delta \delta_m + D_3 = 0. \quad (S-5.3)$$

Here κ , L , A , B , C , D are functions of m .

$$m = 0, 1, \dots, M-1 \quad \text{in (1) and (2);} \quad m = 1, 2, \dots, M-1 \quad \text{in (3).}$$

Boundary conditions.

Lower: σ_0 is given (or $U_0 = 0$),

T_0 is given,

(S-6)

Upper: $T_M - T_{M-1} = 0, \quad u_M - 2u_{M-1} + u_{M-2} = 0.$

The algorithm we used for solving the problems (S-5, S-6) consist of the following steps.

Step One

It is assumed** that as a consequence of the boundary condi-

*In each iteration "according to 1" numbers containing v_ψ in (6) and (9) are taken from the afore-mentioned iteration.

** It is easily shown that as a consequence of the boundary condition $T_u = T_{u-1}$, there are three relations connecting U , T , $\sigma|_{m+1}$ and U , T , σ/m . The possibility of solving them for U , T , $\sigma|_{m+1}$ is already assumed.

tion $T_u = T_{u-1}$, there are the following three relations (cf. S-4):

$$\begin{aligned} U_{m+1} &= \alpha_1(m)U_m + \beta_1(m)T_m + \gamma_1(m)\sigma_m + \delta_1(m), \\ T_{m+1} &= \alpha_2(m)U_m + \beta_2(m)T_m + \gamma_2(m)\sigma_m + \delta_2(m), \\ \sigma_{m+1} &= \alpha_3(m)U_m + \beta_3(m)T_m + \gamma_3(m)\sigma_m + \delta_3(m). \end{aligned}$$

Inserting them in (S-5) it is not difficult to obtain recurrent relations expressing L, B, γ , δ/m as α , B, γ , $\delta/m-1$. As initial values for $m = U-1$ we have:

/36

$$\alpha_2(U-1)=0, \quad \beta_2(U-1)=1, \quad \gamma_2(U-1)=0, \quad \delta_2(U-1)=0.$$

The remaining coefficients for $m = u-1$ are easily found from equations (S-5.1) and (S-5.2) for $m = u-1$. Thus the first step consists of successively finding α , β , γ , δ , from $m = u-1$ to $m = 0$.

Step Two

As a consequence of the boundary condition and the relation (S-7), there is the following connection between the quantities in one point.

$$\alpha_4(m)U_m + \beta_4(m)T_m + \gamma_4(m)\sigma_m + \delta_4(m) = 0. \quad (S-8)$$

The coefficients α_4 , β_4 , γ_4 , δ_4 are also easily found in recurrent form from $m = u-2$ to $m = 0$.

In the third step, from relation (S-8) and the two lower boundary conditions, σ_0 is found.

Of course, in the fourth step from the recurrent formula (S-7) the successively found U , T , σ for all $m = 1, 2, \dots, U$. The analog of the algorithm described from the "die" method for equations (S-3) is obvious.

5. We shall interpret the described algorithm in the spirit of the considerations of paragraph 1. The system (S-5) has in the aggregate four orders. Its solution is completely determined by its values in points m and $m+1$, however these values may not be assigned arbitrarily: (S-5.1) and (S-5.2) yield two connections.

*Translation Note: Original text fails to label S-7

We shall introduce the 6-dimensional space:

$$R^6(x_m) = \begin{vmatrix} U_m & U_{m+1} \\ T_m & T_{m+1} \\ \sigma_m & \sigma_{m+1} \end{vmatrix}$$

/37

All solutions of (S-5) contain in them the 4-dimensional hyperplane of the given equations (S-5.1) and (S-5.2).

Those solutions of (S-5) which satisfy the condition $T_u = T_{u-1}$ are contained in $R^6(x_m)$ of the three-dimensional hyperplane $R_+(x_m)$.

(S-7) is an equation of this hyperplane. In the selected form of notation of these equations is the assumption that the coefficient for U , T , $b/m+1$ do not go to zero.

Solutions satisfying the two upper boundary conditions are contained in the $R^6(x_m)$ two-dimensional hyperplane $R^2_+(x_m)$. It should be assigned by four equations.

As such, we have chosen (S-7) and (S-8). Thus, the first two steps are the "transfer of boundary conditions" from upper to lower.

Step three is the use of lower boundary conditions.

The fourth step is finding the unknown. In this we automatically find ourselves for each m in $R^3_+(x_m)$, but (S-8) is not used and could be violated in terms of errors of curvature. In our calculations the boundary condition $U_u - 2U_{u-1} + U_{u-2} = 0$ was accurately fulfilled, i.e. this possibility was not realized.

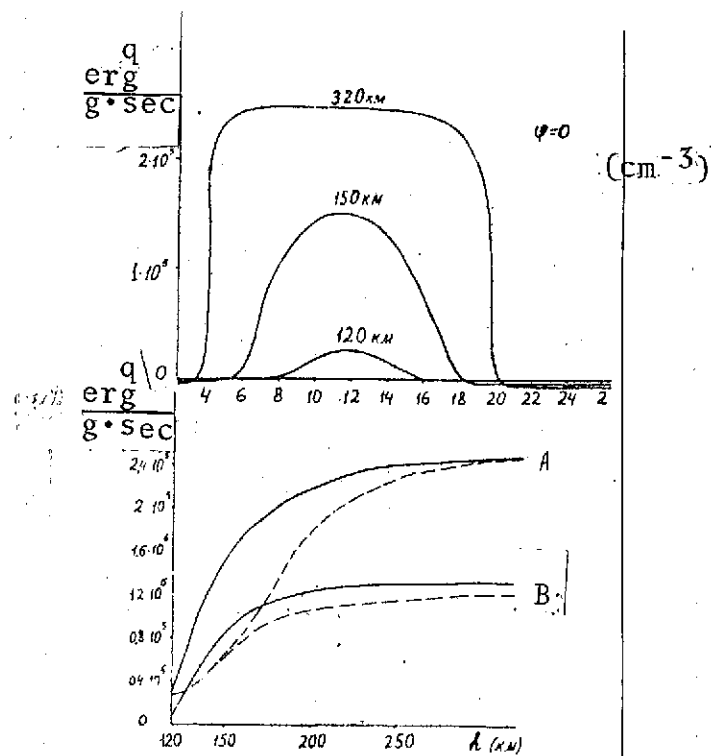
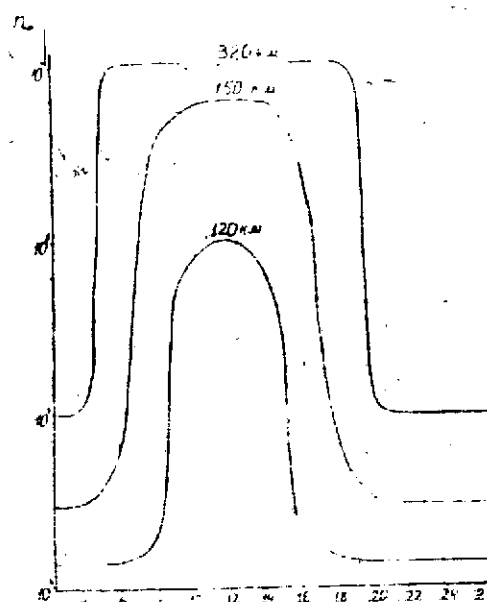


Fig 1. Function of thermosphere heating $q = Q_{ST} - Q_{TR}$ as a func-

tion of time of day and of altitude. The solid curve is according to the exact formula; the dotted curve to the approximate formula. A: according to flux of solar radiation for average solar activity $F_{10.7} = 150 \cdot 10^{-22} \frac{\text{watts}}{\text{M}^2 \cdot \text{Hz}}$

B: during low solar activity (flux in an ionization continuum (30-1050Å) one half of A.



Local time (hrs)

Fig. 2. A simplified function of electron concentration upon time of day, taken for the calculation of ion friction.

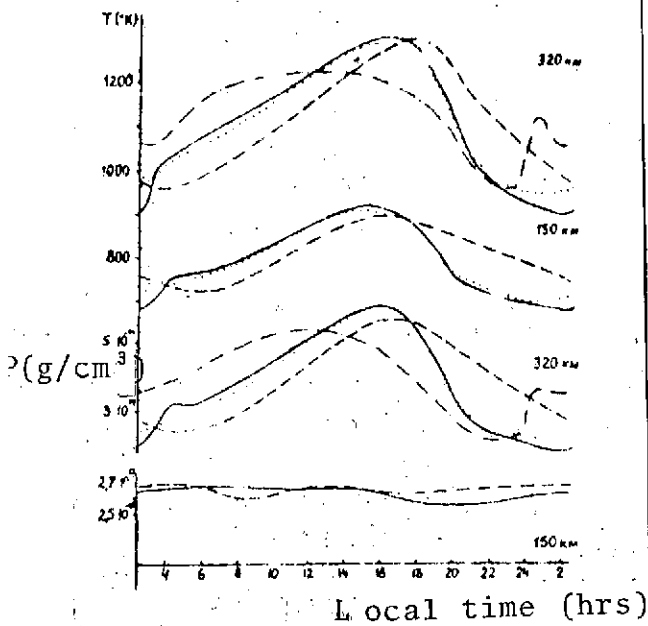


Fig.3. Diurnal variations of temperature and atmospheric density at altitudes of 150 and 320 km during high solar activity.

- basic variant
- - - - - ion friction less than 10 times
- no horizontal motions ($U\psi = 0$)
- introduction of additional viscosity.

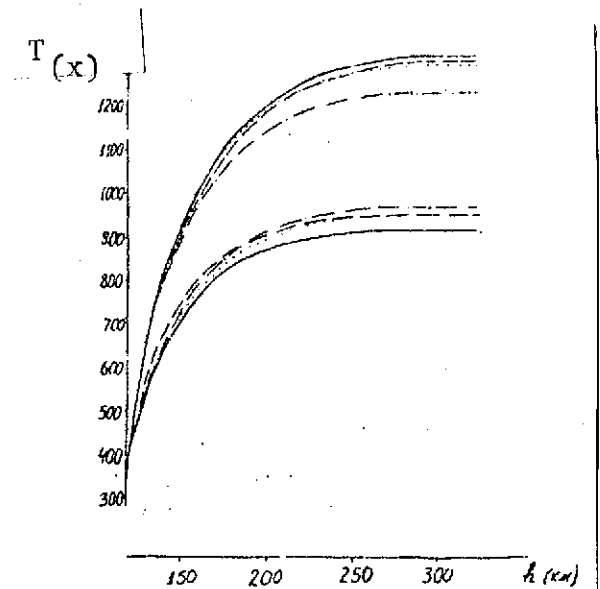


Fig. 4a

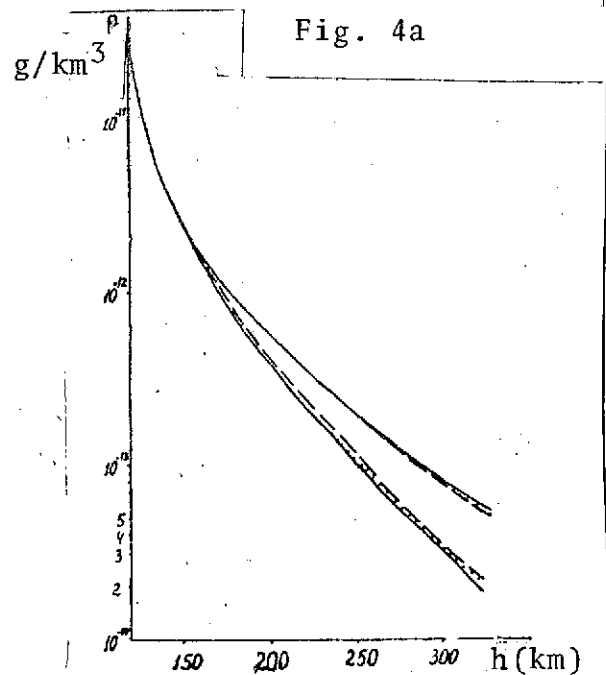


Fig. 4b

Fig. 4. Altitude profiles of temperature (a) and density (b) of the atmosphere. Notation same as for Fig. 3.

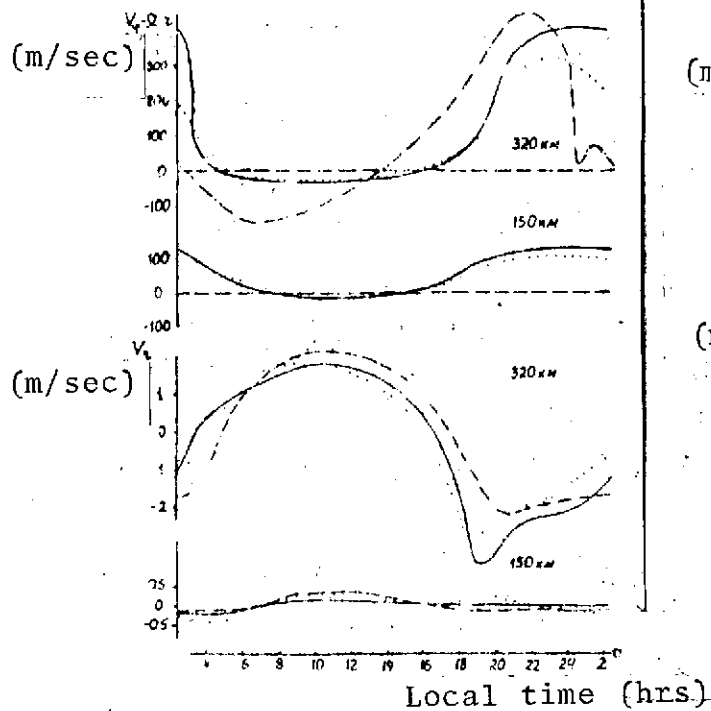


Fig. 5. Diurnal variations of winds at altitudes of 150 and 220 km during high solar activity. Notation same as for Fig. 3.

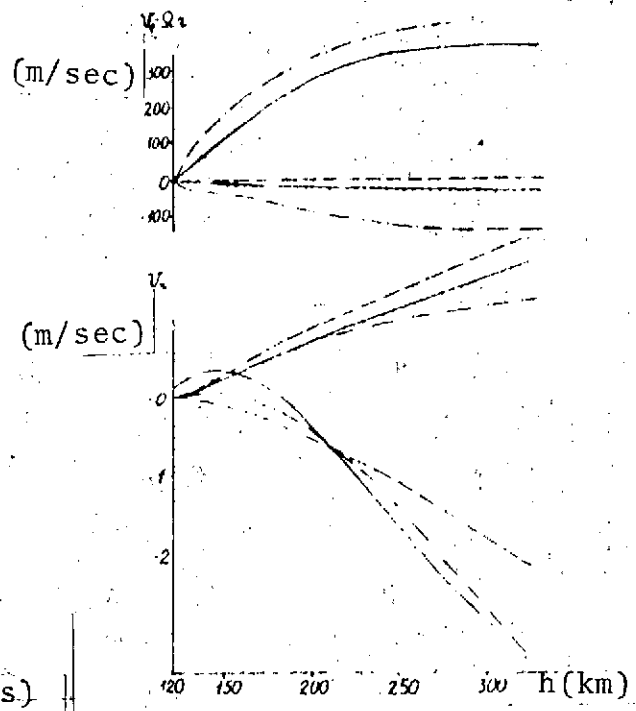


Fig. 6. Altitude profiles of wind during high solar activity. Notation same as for Fig. 3.

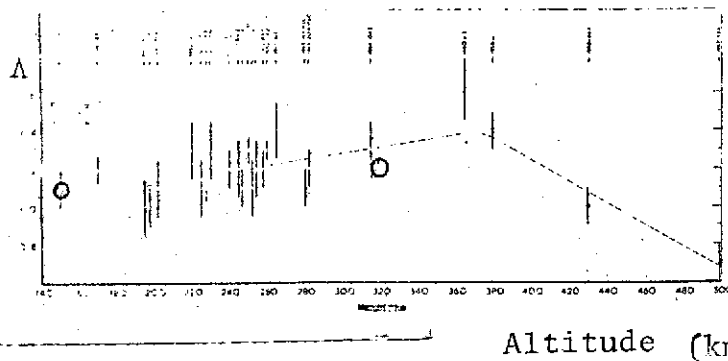


Fig. 7. Ratio of velocity of rotation of atmosphere to velocity of its rotation together with the earth $\Lambda = \frac{\Omega_1 + \bar{v}\psi}{\Omega_1}$

\emptyset = results of King-Hele measurements
 0 = results of calculation.

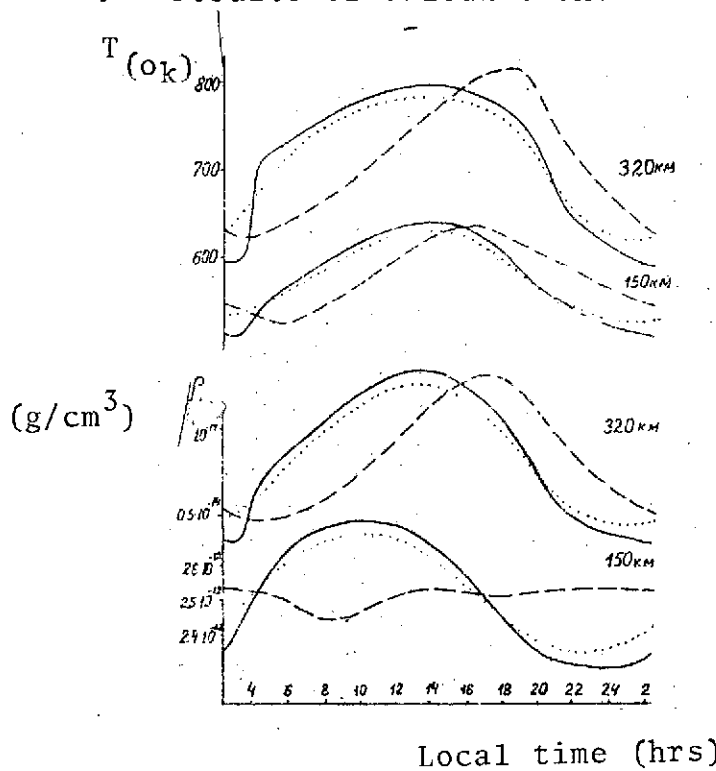


Fig. 8. Diurnal variations of atmosphere temperature and density at altitudes of 150 and 320 km during low solar activity. Notation same as for Fig. 3.

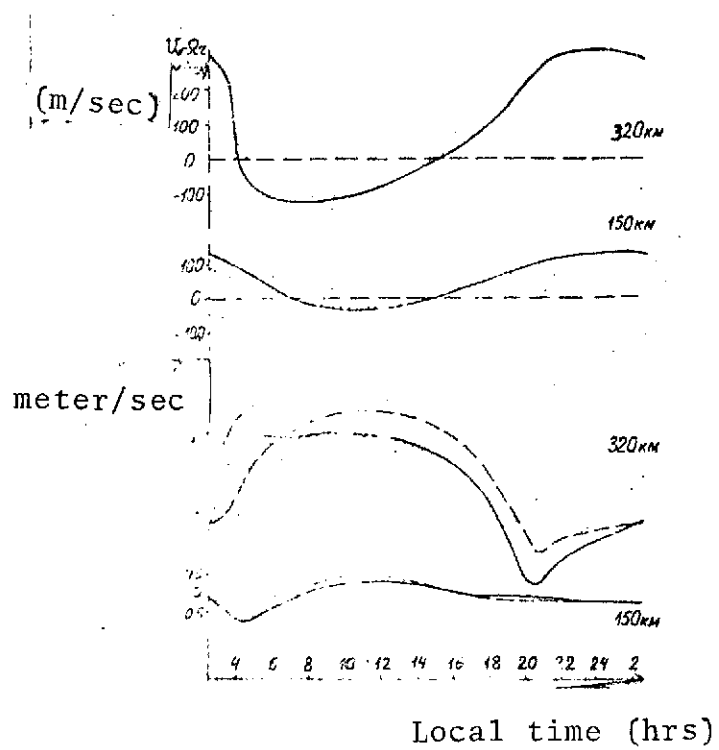


Fig. 9. Diurnal variations of winds at altitudes of 150 and 320 km during low solar activity. Notation same as for Fig. 3.

1. Harris, I. Priester, W.: J. Atmos. Sci., 1962, 19, 286; 1965, 22, 3.
2. Lagos, C.P., Mahoney, J. R.: J. Atmos. Sci., 1967, 24, 88.
3. Friedman, M.P.: Smithson Astrophys. Observ. Spec. Rep., 250, 1967.
4. Geisler, J. E.: J. Atmos. Terr. Phys., 1966, 28, 703; 1967, 29, 1469.
5. Lindzen, R.S.: J. Geophys. Res., 1966, 71, 815; 1967, 72, 1591.
6. Kohl, H., King, J.W.: J. Atmos. Terr. Phys., 1967, 29, 1045.
7. Challinor, R.A.: Planet. Space Sci., 1969, 17, 1097; 1970, 18, 1485.
8. Ivanovskiy, A.N., Repnev, A.N., Shvidkovskiy, Ye. G., Kinetic Theory of the Upper Atmosphere, Leningrad, 1967.
9. Priester, W., Roemer, M., Volland, H.: Space Sci. Reviews, 1967, 6, 707.
10. Izakov, M.N.: Reports of the USSR Acad. Sci., 1967, 177, 1324.
11. Izakov, M.N.: Space Sci. Reviews, 1967, 7, 579.
12. Izakov, M.N.: Space Sci. Reviews, 1971, 12, 261
13. Volland, H.: Space Research VII, 1967, 1193
14. Dickinson, R.E., Lagos, C.P., Newell, R.E.: J. Geophys. Res. 1968, 73, 4200.
15. Volland, H., Mayr, H.G.: Ann. Geophys., 1970, 26, 907.
16. Izakov, M.N., Morozov, S.K., Shnoll, E.E.: Space Research XII, 1972.
17. Friedman, M.P.: Smithson Astrophys. Observ. Spec. Report 316, 1970.
18. Harris, I., Priester, W.: Meteorolog. Monographs, 1968, 9, 72.
19. Izakov, M.N.: Geomagnetism and Aeronomy, 1970, 10, 283.
20. Izakov, M.N., Morozov, S.K.: Geomagnetism and Aeronomy, 1972, 1970, 10, 630.
21. Izakov, M.N., Morozov, C.K., Krasitskiy, O., Yashchenko, I.A.: Geomagnetism and Aeronomy, 1972, in press.
22. Johnson, F.S., Gottlieb, B.: Planet. Space Sci., 1970, 18, 1707.
23. Bates, D.R.: Proc. Phys. Soc., 1951, 364, 805.
24. Shvëd, G.M., Nerushev, A.F.: Isv. AN SSSR, Phys. Atmos. i Okeana, 1969, 5, 473.
25. Kockarts, G., Petermans, W.: Planet. Space Sci., 1970, 18, 271.
26. Blamont, J.S., Luton, J.M.: Paper presented at COSPAR Meeting, 1971, Seattle.
27. Hines, C.O., J. Geophys. Res., 1965, 70, 177.
28. Lindzen, R.S., Blake, D.: J. Geophys. Res., 1970, 75, 6868.
29. Roper, R.G.: Paper presented at IUGG General Assembly, 1971, Moscow.
30. Feier, J.A., in collection on Physics of the Upper Atmos. of the Earth, Leningrad, 1971, 168.
31. Rishbeth, H., Garriott, O.K.: Introduction to Ionospheric Physics, 1969
32. Chapman, S., Cauling, T. Mathematical Theory of Inhomogenous Gasses, Moscow, 1960.
33. Braginskii, S.I., in collection Theory of Plasma, I, Moscow, 1963.

34. Banks, P.: Planet Space Sci., 1966, 14, 1105.
35. Stubbe P.: J. Atmos. Terr. Phys., 1968, 30, 1965
36. Nisbet, J.S.: Pennsylvania State Univ. Sci. Report 355, 362E, 1970.
37. COSPAR International Reference Atmosphere CIRA-65, Amsterdam 1965.
38. Jacchia, L.G.: Smithson. Astrophys. Observ. Spec. Report, 332, 1971.
39. Hinteregger, H.E.: Ann. Geophys. 1970, 26, 547.
40. Ivanov-Kholodniy, G.S., Nikol'skiy, G.M.: Sun and Ionosphere, Moscow, 1968.
41. Blum, P., Harris, I., Priester, W. in CIRA-72, 1972.
42. Waldeufel, P., Cogger, L.: J. Geophys. Res., 1971, 76, 5322.
43. Izakov, M.N., Yashchenko, I.A.: Geomagnetism and Aeronomy, 1972.
44. Izakov, M.N., Morozov, S.K., Jaschenko, I.A.: Paper presented at COSPAR Meeting, 1972.
45. King-Hele, D.G.: Planet.Space Sci., 1964, 12, 835.
46. King-Hele, D.G.: Nature, 1971, 233, 325.
47. King-Hele, D.G.: Space Res., X, 1970, 537.
48. Kolesnikova, V.N., Monin, A.S.: Isv. AN SSSR, Phys. Atmos. i Okeana, 1965, 653.
49. Monin, A.C., Obukhov, A.M.: in collection Dynamics of Large-Scale Atmospheric Processes, Moscow, 1967, 194.
50. Godunov, S.K.: Uspechi Matematich. Nauk, 1961, 16, 171.
51. Godunov, S.K.: Zhurn. vychislit. Matem. i Matem.Phiziki, 1962, 2, 972.
52. Godunov, S.K. Uravneniya Matem.Phiziki, Moscow, 1971.